

19.5% EFFICIENT N-TYPE SI SOLAR CELLS MADE IN PRODUCTION

A.R. Burgers¹, L.J. Geerligs¹, A.J. Carr¹, A. Gutjahr¹, D.S. Saynova¹, Xiong Jingfeng², Li Gaofei²,
Xu Zhuo², Wang Hongfang², An Haijiao², Hu Zhiyan², P.R. Venema³, A.H.G. Vlooswijk³

¹ECN Solar Energy, P.O. Box 1, NL-1755 ZG Petten, the Netherlands
Phone: +31 224 56 4959; Fax: +31 224 56 8214; email: burgers@ecn.nl

²Yingli Solar, 3399 Chaoyang North Street, Boading, China

³Tempress Systems BV, Radeweg 31, 8171 Vaassen, The Netherlands

ABSTRACT: We present the status of our process development of silicon solar cells on n-type base material, and progress towards its industrial implementation. Independently confirmed efficiencies for Cz of 19.5% (239 cm²) have been obtained. To our knowledge these are the highest industrial scale efficiencies obtained with processing based on homogeneous emitter and screen-printing. We present an update of our process development, including efficiency improvements.

Keywords: n-type, Silicon, High-Efficiency

1 THE CASE FOR N-TYPE SILICON CELLS

Currently, more than 85% of the solar cells produced worldwide are based on crystalline silicon [1]. The fraction of crystalline silicon cells made from p-type material is close to 95%, and only somewhat more than 5% is made from n-type material. Although the total production of n-type crystalline silicon solar cells is limited, two top-10 players, SunPower [2] and Sanyo [3], are using this material to manufacture high-efficiency solar cells. Both manufacturers apply advanced technologies and use high-quality monocrystalline base material. SunPower is manufacturing fully back-contacted cells (Interdigitated Back-Contacted, IBC) and Sanyo is producing so-called HIT (Heterojunction with Intrinsic Thin-layer) cells. On both cell types efficiencies of 23% have been reached. For the HIT cells both emitter and back-surface-field (BSF) are formed by the deposition of thin doped amorphous silicon layers. The surface passivation is accomplished by a layer of intrinsic amorphous silicon with a thickness of just a few nm.

The use of n-type material has several advantages over the use of p-type. Firstly, n-type material is less sensitive to most common metallic impurities, like Fe [4,5,6]. Because of this n-type material could have a higher tolerance for lower-quality feedstock [7,8]. Also after gettering and passivation higher minority carrier diffusion lengths have been observed for n-type material. Secondly, in n-type material there is no boron dopant, and hence boron-oxygen defects will not be formed. This defect is formed upon illumination in p-type Cz silicon, degrading the bulk lifetime of the material. Therefore n-type Cz will not suffer from Light Induced Degradation [9,10].

2 N-TYPE SILICON SOLAR CELLS ISSUES

There are numerous challenges that have to be dealt with when processing n-type material into solar cells. One challenge is the formation of p-type emitters by boron diffusion. Boron diffusion requires much higher temperatures than conventional phosphorous diffusion. This will make the simultaneous formation of the emitter and BSF a challenge.

A second challenge is the passivation of these highly-doped p-type emitter regions. Thermal oxidation is an option, but requires a long and high-temperature process step. A single-layer SiN_x coating will not result in good surface passivation because of the positive fixed charges

in the layers. The positive fixed charges will not lead to accumulation like in p-type Si, but will cause a tendency towards depletion in which the pn-product will increase and consequently the surface recombination will increase. Another issue is finding a suitable metallization for the boron doped emitter.

ECN has a long standing experience in developing processes for multi-crystalline silicon solar cells. In these developments the transfer towards industry is always born in mind. This has led to several successful industrial processes, such as acid texturing of multi-crystalline silicon, and industrial application of the PECVD silicon nitride. The aim for the n-type process was to develop a process that would have a potential for large scale production.

3 ECN'S N-TYPE CONCEPT

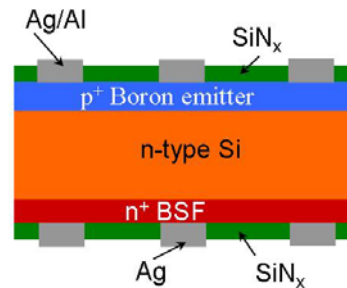


Figure 1: structure of the n-type cell

The structure of the fabricated n-type cells is illustrated in Figure 1. The rear side of the cells is passivated by a phosphorous back-surface field and a SiN_x layer. The rear side metallization has an open structure that can enhance the internal reflection. The front side of the cell has a boron emitter, passivated with silicon nitride. The boron emitter is contacted with silver-aluminium metallisation.

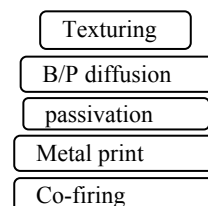
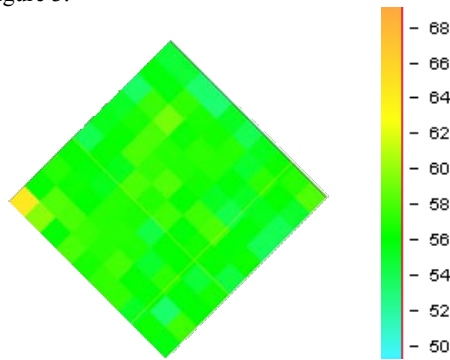
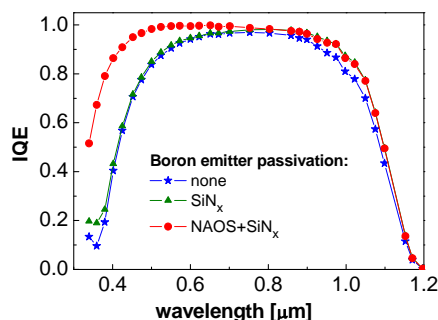


Figure 2: Schematic process order

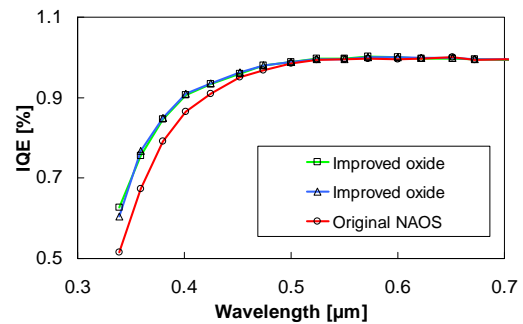
The process is executed on semi-square 6 inch n-type CZ wafers and is given schematically in Figure 2. The first step is a texturing the wafers with random pyramids using alkaline etching. The boron emitter and the phosphorous BSF were formed in a co-diffusion step using an industrial tube furnace [12] from Tempress. A 60 Ω /sq emitter is made using BBr_3 . We are able to make boron emitters with a standard deviation in sheet resistivity of about 1.5 Ω /sq [12]. A sheet resistance scan can be seen in Figure 3:

**Figure 3:** Sheet resistance mapping of a 60 Ω /sq boron emitter.

Surface passivation of the highly-doped boron emitter was performed using a simple and patented wet chemical oxidation process [13,14]. SiN_x layers for ARC and passivation purposes were deposited using our Roth&Rau PECVD system. The effect of using an oxide layer with a PECVD SiN_x ARC layer can be seen in Figure 4.

**Figure 4:** Internal quantum efficiency of cells with and without intermediate oxide layer.

It is clearly visible that the blue response of cells with a silicon oxide passivating layer is much better than that of cells without oxide and only a single SiN ARC layer, which is explained by reduction of the interface charges at the silicon nitride – silicon interface. Recently, we have improved our wet oxide passivation process even further resulting in a gain in V_{OC} of about 10 mV [15]. The internal quantum efficiencies of both passivating oxide layers are presented in Figure 5.

**Figure 5:** Internal quantum efficiency of cell with original NAOS oxide passivation and IQE of two cells with improved wet chemical oxidation.

For the passivation of the p+ emitter there are more methods available, with coating by Al_2O_3 via atomic layer deposition (ALD) receiving much attention in literature [16,17]. Several companies are actively developing equipment for PV industry to deposit Al_2O_3 (by ALD) or AlO_x (by e.g. PECVD).

Screen-printing was used to apply front and rear side Ag metallization. We used a co-firing step to sinter the metallization pastes and form an electrical contact to the diffusion.

Cells made with this process have a combination of features, that makes them very attractive for industrial implementation.

- The cell is bifacial. This feature can be exploited in bifacial modules to generate additional electricity.
- A phosphorous BSF is used on the rear. The BSF provides additional lateral conductivity at the rear side. This results in a good fill factor despite the open rear side metallization.
- There is no aluminium BSF, and hence no bending of the cells.
- The n-type material results in a good efficiency
- We use homogeneous diffusions at front and rear side, no selective processes, keeping the process relatively simple.
- There is a good passivation of the rear surface.
- We use processing steps that can be executed on an industrial scale.
- The metallization has several benefits
 - The metallization at front and rear side is open, hence we have a limited coverage and paste usage. Ag use on the rear is only slightly higher than for the contacting Ag pads on Al-rear side mainstream cells.
 - The metallization can be applied with regular screen printing.
 - The pastes we employ are solderable pastes, no additional print is required to obtain a solderable cell.

4 TRANSFER TO INDUSTRY

The process was developed in ECN's pilot line. In June 2009, ECN, Amtech Systems, and Yingli Green Energy announced a three party research agreement, to further industrialize and develop the n-type open rear side cell. The project was soon dubbed "Panda". For Yingli the Panda technology presented a unique opportunity to enter the market with a product that differs from the mainstream of multi-crystalline silicon technology. For Tempres the project allows to develop its diffusion technology and product port-folio for the PV industry. For ECN, the project allows accelerated development of the technology.

ECN drafted specifications and requirements for a pilot line. Based on these specifications Yingli adapted an existing facility for execution of the Panda process. The adaptation of the pilot line did not involve major capital expense, as the Panda process required only moderated changes to the pilot line.

Based on the specifications Yingli was able to get the process running even before the first ECN personnel arrived on site. An extensive experimental program was executed to tune and improve the process. The capacity of the pilot line and commitment of the team allowed to execute this program at a very rapid pace, leading to good results. Also the connections and weight of Yingli as major solar cell manufacturer helped to accelerate developments at equipment- and materials suppliers. The efficiency has progressed over time. There are several factors contributing to the steady increase in efficiency. One gets better at processing these cells as one processes more cells, and the processing is tuned and gets more stable. This effect is big since a dedicated pilot line has been in operation at Yingli. The best independently confirmed (ISE Callab) efficiency is 19.5% (on 239 cm²). These promising results lead Yingli to announce a 300MW production of Panda cells in March 2010.

5 TOWARDS HIGHER EFFICIENCY

The current Panda cell design has room for improvement, as was shown in an experiment with a different BSF.

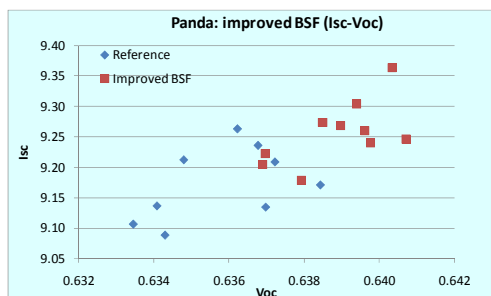


Figure 6: Gain in current and voltage because of an improved BSF.

In Figure 6 the effect on current and voltage of this BSF is shown. In Table 1 the complete set of I-V parameters is shown. The last column η^* shows a theoretical efficiency, assuming an identical fill factor of 79.1% for both groups. From this column we see that a gain of 0.3% absolute in efficiency is possible due to improvement of the product of current and voltage. The challenge of course is to maintain the fill factor with this BSF.

Table 1: I-V parameter for cell with new BSF.

group	I_{sc} (A)	V_{oc} (V)	FF (-)	η (%)	η^*
ref	9.17	0.636	0.791	19.31	19.30
Improved BSF	9.26	0.639	0.741	18.35	19.57

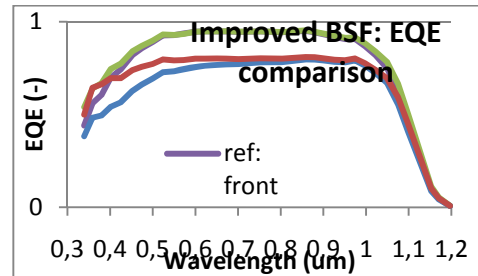


Figure 7: EQE comparison for different BSF.

Figure 7 shows a comparison of the quantum efficiencies. Since the Panda cells have an open rear side, the quantum efficiency can be measured from both front- and rear side. The blue response at the rear side is improved for the new BSF compared to the reference. The improved blue response at the rear side is an indication of reduced recombination at the rear side, and leads to an improvement of the red response from the front side. A second topic where gains can be realized is in contact recombination.

Table 2: Impact of metallization on voltage

Sample stage	V_{oc} or implied V_{oc} (mV)
No metallization	652
Rear metallization	642
Front- and rear metal	632

In Table 2 the voltage of samples was compared with- and without metallization. The sample without metallization has had complete processing including firing, but does not have the metallization prints. For all samples the implied V_{oc} was measured using QSSPC (Quasi Steady State Photo Conductance). For the sample with front- and rear metal the voltage can in addition be determined by Suns- V_{oc} and I-V measurements.

Table 3: J_0 values and V_{oc} impact for front metal.

Current value fA/cm ²	Impact on cell J_0 fA/cm ²	Impact on V_{oc}
$J_0: \sim 3350 \pm 350$	240 ± 25 for 7.5% coverage	$\sim 10 - 15$ mV 1.3-2.0 mV per % of metal

From these and other measurements, we have obtained estimates of the saturations currents of surfaces and metal contacts. For a particular surface we assume that the total saturation current is an area weighted average of the saturation currents of the contacted and uncontacted areas. Table 3 shows the impact of the front metal contact on the voltage. Because of the high saturation current, the contacts have a significant impact despite a limited coverage fraction.

Table 4: Impact of reduced contact area on voltage

Metallization scheme	I_{sc} (A)	V_{oc} (V)	FF (%)	η (%)
Reference	9.03	0.629	77.3	18.37
Reduced contact area	9.02	0.633	77.1	18.44

Table 4 shows results of an experiment in which the metal coverage fraction with reduce with 3%. The increase in cell voltage is consistent with the numbers from Table 3.

6 CONCLUSIONS

Using n-type base material can lead to higher efficiencies thanks to its lower sensitivity to most common metallic impurities and the absence of boron-oxygen complexes. Up to now only SunPower and Sanyo are able to manufacture cells with efficiencies above 20% on industrial scale (using n-type material). They use, however, advanced processing.

Issues when processing n-type solar cells are boron diffusion and passivation of the highly doped boron emitter. We have developed an industrially feasible process using standard manufacturing equipment for boron-phosphorous co-diffusion and passivation of both diffusion. With these low-cost technologies we are able to make 19.5% (independently confirmed) efficient cells on large 239 cm² area.

We think the Panda process strikes a good balance between efficiency and manufacturability, and has the potential to become a viable competitor within the range of technologies already available and those being on the verge of entering the market. However development on the technology will have to continue.

7 REFERENCES

- [1] Photon International March 2009, p170.
- [2] us.sunpowercorp.com
- [3] www.sanyo.com/solar
- [4] D. Macdonald and L.J. Geerligs, Appl. Phys. Lett. (2008) 92 p4061.
- [5] J.E. Cotter et al., 15th Workshop on Crystalline Silicon Solar Cells & Modules: Materials and Processing 2005, p3.
- [6] N. Guillevin et al. 19th Workshop on Crystalline Silicon Solar Cells & Modules: Materials and Processes 2009, p26.
- [7] A. Cuevas et al., Appl. Phys. Lett. 81 (2002) p4952.
- [8] S. Martinuzzi et al., Progr. Photovolt.: Res. Appl. 17 (2009) p297.
- [9] J. Schmidt et al. 26th IEEE PVSC Anaheim, 1997, p13.
- [10] S. Glunz et al., 2nd WCPEC Vienna 1998 p1343.
- [12] Y. Komatsu, Solar Energy Mat. & Solar Cells 93 (2009) p750 (17th PVSEC, 2007, Fukuoka).
- [13] V.D. Mihailetchi et al., Appl. Phys. Lett. 92 (2008) p63510, patent WO08039067.
- [14] V.D. Mihailetchi et al., 22nd EPVSEC Milan 2007, p837.
- [15] R. Naber et al., 34th IEEE PVSC, 2009.
- [16] B. Hoex et al., Appl. Phys. Lett. 89 (2006) p042112.
- [17] B. Hoex et al., Appl. Phys. Lett. 91 (2007) p112107.